Electronic stopping in insulators: a simple model

2007 J. Phys.: Condens. Matter 19 275211

(http://iopscience.iop.org/0953-8984/19/27/275211)

IOP PUBLISHING JOURNAL OF PHYSICS: CONDENSED MATTER

J. Phys.: Condens. Matter **19** (2007) 275211 (10pp) doi:10.1088/0953-8984/19/27/275211

Electronic stopping in insulators: a simple model

Emilio Artacho

Department of Earth Sciences, University of Cambridge, Downing Street, Cambridge CB2 3EQ, UK
and
Donostia International Physics Centre, Universidad del País Vasco, 20080 San Sebastián, Spain

E-mail: emilio@esc.cam.ac.uk

Received 14 March 2007, in final form 3 May 2007
Published 1 June 2007
Online at stacks.iop.org/JPhysCM/19/275211

Abstract

A simple model is presented to explore, review and illustrate basic concepts related to the electronic stopping power in large electronic band gap insulators. A projectile shooting through the solid is described by a local potential $V(\mathbf{r} - \mathbf{v}t)$. The flat band limit is assumed for both valence and conduction bands. The energy-transfer rate is calculated by solving the time-dependent quantum mechanics for the timescale of electron excitation near the trajectory, taking the timescale for electronic energy out-diffusion to be much larger. The threshold effect in the low projectile velocity limit is characterized.

(Some figures in this article are in colour only in the electronic version)

1. Introduction

In the physics of ions moving through solids [1, 2] it is customary to differentiate between the energy transferred by the projectile to nuclear motions, the rate of which is called the nuclear stopping power, and the energy transferred to electronic excitations, giving the electronic stopping power. The distinction is relevant since the different masses of nuclei and electrons give rise to different response regimes: the nuclear stopping power dominates at lower projectile velocities, while the electrons respond more readily at higher speeds. It is also a convenient decoupling, since two limits can be studied and understood more easily: electronic excitations for frozen nuclei, in the high-velocity regime, and atomic motions with electrons following adiabatically in the slow regime. Intermediate cases are, as ever, harder to describe. Such is the situation encountered when facing the damage produced in materials when subjected to radioactive decay processes.

An alpha decay of a heavy nucleus produces an alpha particle shooting through the host material with a kinetic energy of ∼5 MeV (velocity ∼ 7 au), whilst the remaining nucleus recoils with ∼100 keV ($v \sim 0.1$ au). The damage produced by the recoiling nucleus has been simulated theoretically in the adiabatic limit [3, 4], since it is known that nuclear stopping

dominates [1]. It has not been established, however, how much electronic stopping there is in these events. It is an important question, since local electronic excitation can substantially alter the interatomic interactions and thus may affect the reliability of the simulations.

Direct experimental knowledge of electronic stopping power at low velocities is hard to obtain, given the larger contribution of the nuclei to the stopping. A better overall understanding of electronic stopping in metals, which predicts a linear dependence with velocity in the slow regime, allows a better characterization [2]. For insulators, however, a threshold effect is expected and has been experimentally observed [5]: a highly nonlinear behaviour very difficult to access experimentally, which prevents any quantitative assessment of the importance of the electronic excitation at the recoil velocities mentioned above. This is of special relevance for the study of the glasses and ceramic materials used and proposed for hosting nuclear waste.

While the electronic stopping power values are being obtained from first-principles time-dependent calculations elsewhere [6], this paper concentrates on qualitative aspects of the expected behaviour by focusing on a simple model obtained in the flat-band limit. It is a different approach from the usual perturbative, linear-response based studies, which have offered important insights, but have been mostly applied to metals and/or weak perturbing potentials [2]. The model allows for a non-perturbative hierarchy of approximations of increasing complexity towards insulating solids. This papers sets the scene by limiting itself to the simplest level, which allows the introduction of several fundamental concepts in an intuitive manner.

There are interesting connections of the following to earlier works in the quantum chemistry community, where there is a long and fruitful history of research on non-adiabatic collisions between atoms [7]. In addition to their different context, this work differs from earlier quantum chemistry work in the fact that it does not need well-defined asymptotic exit channels, since the excitations induced by the projectile in a solid find an infinity of thermalization channels. The model is introduced in section 2 as well as the main approximations, and some results are presented and discussed in section 3.

2. Model

The electronic structure of the host material is described by dispersionless valence and conduction bands separated by a band gap E_{g},

$$H_{\mathrm{o}} = \varepsilon \sum_{i,\sigma} n_{\mathrm{v},i,\sigma} + (\varepsilon + E_{\mathrm{g}}) \sum_{i,\sigma} n_{\mathrm{c},i,\sigma} \tag{1}$$

where v and c stand for valence and conduction states, respectively, and i runs over localized Wannier-like states. Valence (conduction) localized states can be visualized as the bonding (anti-bonding) states for each bond in a covalent solid, or states localized on the anions (cations) in an ionic solid. Only one valence band and one conduction band are considered. The effect of going beyond this flat-band approximation will be explored in section 3 only for the results obtained through perturbation theory. An effective one-particle picture will be used throughout, disregarding self-consistency and electronic correlation effects.

Assuming for simplicity a local, spin-independent potential, $V(\mathbf{r})$, to describe the projectile, its effect on the electrons as it moves through the solid with a given velocity, $\mathbf{v}$, is described by $V(\mathbf{r} - \mathbf{v}t)$, and thus,

$$H = H_{\mathrm{o}} + \sum_{i,j,\sigma} \left[V_{i,j}(t) c^{\dagger}_{\mathrm{c},i,\sigma} c_{\mathrm{v},j,\sigma} + \mathrm{h.c.} \right], \tag{2}$$

where the c–c and v–v hybridizations have been neglected, and where

$$V_{i,j}(t) = \int \mathrm{d}^3\mathbf{r}\psi^*_{\mathrm{c},i}(\mathbf{r})V(\mathbf{r}-\mathbf{v}t)\psi_{\mathrm{v},j}(\mathbf{r}), \tag{3}$$

i.e., a convolution of the local overlap of valence and conduction functions with the moving potential. The inclusion of c–c and v–v hybridizations would represent a dynamical redefinition of the localized (eigen)states, which, at the level of this analysis, can be thought of as redefining $V_{i,j}(t)$. The c–c and v–v hybridizations on their own do not produce excitation: the energy changes while the projectile passes, but the system never leaves the adiabatic ground state and thus goes back to the unperturbed ground state after the passage of the projectile.

The basic question is, starting from an initial situation of filled valence band and empty conduction band, what will be the rate of energy transfer from the projectile to the electrons. This can be addressed by following the explicit dynamics of the N electrons described by the Hamiltonian of equation (2), i.e., solving $H|\Psi(t)\rangle = \mathrm{i}\hbar\partial|\Psi(t)\rangle/\partial t$ with $|\Psi(0)\rangle = \prod_{\mathrm{v},i,\sigma} c^\dagger_{\mathrm{v},i,\sigma}|0\rangle$. For independent particles this is equivalent to following the dynamics of each one of the initially occupied one-electron states. The same language is maintained within mean-field-like approximations, like in time-dependent Kohn–Sham theory [8], except that the time-dependent potential depends on the states and their evolution. The solution allows obtaining $E(t) = \langle\Psi(t)|H(t)|\Psi(t)\rangle$, and $S = \frac{1}{v}\frac{\mathrm{d}E(t)}{\mathrm{d}t}$ gives the stopping power as conventionally expressed (energy per unit length).

Two further simplifications are assumed. Firstly, the velocity is taken to be a constant, given the very small stopping that occurs in the length scales considered in this work (stopping powers of $\sim$1 eV Å^{-1} over a few Å imply negligible changes in velocity if the incoming kinetic energy is $\sim$100 keV). The system becomes non-conservative, however. The second approximation is more drastic: it is assumed that any one valence state substantially overlaps with only one conduction state, rendering other pairings negligible. Assuming one to one regularity, v–c pairs will be labelled with the same i index.

This extremely simplified model becomes a collection of non-interacting two-state subsystems. As the projectile moves it excites the subsystems within its potential range. Subsystem i sees a time-dependent potential that takes it from $|\psi_i(0)\rangle = |\psi_{\mathrm{v},i}\rangle$ to

$$|\psi_i(t)\rangle = \mathrm{e}^{-\mathrm{i}\varepsilon t/\hbar}\left(\alpha_i|\psi_{\mathrm{v},i}\rangle + \mathrm{e}^{-\mathrm{i}E_\mathrm{g}t/\hbar}\beta_i|\psi_{\mathrm{c},i}\rangle\right), \tag{4}$$

for long enough times after the passage of the projectile. The projectile leaves the subsystem with a final excitation energy of $|\beta_i|^2 E_\mathrm{g}$ for each spin (we shall drop the spin dependence henceforth for simplicity). The value of β_i depends on the whole history of the passage and can be obtained by integrating the dynamics.

The excitation energy is expected to equilibrate away into the solid at longer timescales. This energy redistribution among subsystems is not explored in this analysis, beyond the fact that it is a conservative process (also involving the system phonons), and that it is unlikely to outrun the projectile i.e., it will define a wake [9]. Our model thus assumes a decoupling of both timescales, excitation and equilibration, which is more justified the narrower the electronic bands. Phonon timescales are indeed much larger. Long-range projectile potentials, however, would not allow such decoupling, since the characteristic duration of the perturbation scales with the range of the potential. Short range is assumed in this paper.

For a crystalline system, the energy transfer per unit length given by this model is stationary by construction, up to an oscillation of period L, the repetition length of the crystal along the projectile direction. For a given (straight) trajectory of the projectile in the crystal, consider a two-dimensionally infinite slab of the crystal, of thickness L, perpendicular to that trajectory. The average stopping power is

$$S = \frac{E_\mathrm{g}}{L}\sum_i^{\mathrm{slab}} |\beta_i|^2 \tag{5}$$

taking the sum over the subsystems associated to the slab. Subsystems closer to the trajectory will feel a larger projectile potential $V_{i,i}(t)$. It will decay with the distance of subsystem i from the trajectory.

The energy absorbed by each subsystem is what needs calculating, by means of solving the time-dependent Schrödinger equation, which becomes

$$\mathrm{i}\hbar\frac{\partial \underline{C}}{\partial t} = H\underline{C} \tag{6}$$

where the subsystem label has been dropped, and with

$$H = \begin{pmatrix} 0 & V(t) \\ V(t) & E_\mathrm{g} \end{pmatrix}, \tag{7}$$

where ε has been taken as 0. The $V(t)$ function can be expressed as $V_\mathrm{o} f(t/\tau)$, where $f(\chi)$ is chosen such that $\max\{|f(\chi)|\} = 1$ (even if $V(\mathbf{r})$ can be divergent, its convolution with sensible localized states will not), and, if short ranged, the characteristic width of $f(\chi)$ is 1, so the characteristic time of passage of V is τ. This time $\tau \propto 1/v$, i.e., increasing velocity narrows the potential $V(t)$, but neither height nor shape are altered.

The parameters of the model are thus E_g, V_o and τ, in addition to the shape of the perturbing potential. Setting the energy scale (e.g. $E_\mathrm{g} = 1$) and having defined the timescale by the energy scale and $\hbar$ (e.g. $\hbar = 1$), the remaining parameters are V_o and the velocity v. Indeed, a rescaling of the velocity (or of τ) is equivalent to a change of energy units, and thus increasing the velocity by α is equivalent to increasing both E_g and V_o by α for the original velocity. If numbers are to be extracted from this analysis, a length scale is needed for a proper definition of velocity. The scale is defined by the characteristic width W of the convolution

$$\left[V \circ \psi_\mathrm{c}^* \psi_\mathrm{v}\right](\mathbf{r}) = \int \mathrm{d}^3\mathbf{r}' \psi_\mathrm{c}^*(\mathbf{r}') V(\mathbf{r}' - \mathbf{r}) \psi_\mathrm{v}(\mathbf{r}') \tag{8}$$

along the direction of the motion of the projectile, i.e., at a velocity v the projectile advances by W in a time τ.

Some of the results presented below have been obtained by numerically solving equation (6). A Crank–Nicholson algorithm has been used for the purpose, in which time is discretized in steps of Δt and the evolution of the coefficients is approximated by

$$\underline{C}(t + \Delta t) = \left[\mathbf{1} - \mathrm{i}\frac{\Delta t}{2}H\right]^{-1}\left(\mathbf{1} + \mathrm{i}\frac{\Delta t}{2}H\right)\underline{C}(t). \tag{9}$$

Converged stable results for the potentials below are achieved with $\Delta t \sim 0.05\hbar/E_\mathrm{g}$.

3. Results and discussion

3.1. Weak perturbation

If the perturbation is weak ($V_\mathrm{o} \ll E_\mathrm{g}$), time-dependent perturbation theory can be used and the problem simplifies extremely, since

$$|\beta|^2 = \frac{1}{\hbar^2}\left|\tilde{V}(\omega = E_\mathrm{g}/\hbar)\right|^2, \tag{10}$$

i.e., the square of the Fourier transform of $V(t)$ evaluated at $\hbar\omega = E_\mathrm{g}$. The velocity dependence enters by scaling the width τ. If $\tau \to \alpha\tau$ (or $v \to v/\alpha$), then $\tilde{V}(\omega) \to \alpha\tilde{V}(\alpha\omega)$, i.e.,

$$|\beta|^2 \propto \frac{1}{v^2}\left|\tilde{V}(\omega \propto E_\mathrm{g}/v)\right|^2, \tag{11}$$

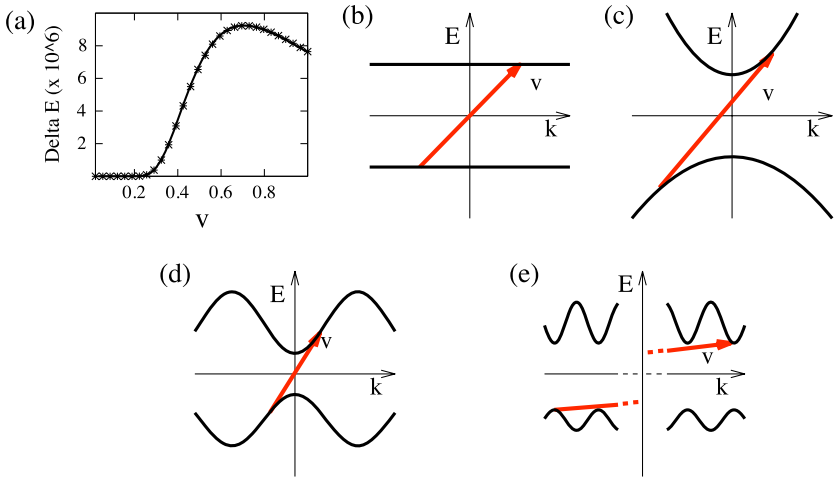

Figure 1. (a) Comparison between the perturbative (symbols; $\Delta E = \pi V_o^2 e^{-\frac{1}{2}\left(\frac{1}{v}\right)^2}/v^2$) and exact solution (line) for the subsystem excitation energy $\Delta E = E_g|\beta|^2$ for a Gaussian potential of amplitude $V_o = 0.002E_g$. Illustration of perturbative transitions induced by a passing projectile of velocity v for dispersionless bands (b), direct band gap parabolic bands (c), and periodic bands, (d) and (e). (c) illustrates a transition for a strict threshold: a larger gap (or smaller v) would prevent stopping completely. (d) shows a similar critical velocity, leading to an abrupt (but incomplete) reduction of stopping at lower v. (e) illustrates the $v \to 0$ asymptotics, made of critical points.

or, specifically,

$$|\beta| = \frac{V_o W}{v\hbar}\left|\tilde{f}\left(\frac{E_g W}{\hbar v}\right)\right| = \frac{V_o}{E_g}\frac{v_o}{v}\left|\tilde{f}\left(\frac{v_o}{v}\right)\right|, \tag{12}$$

$\tilde{f}$ being the Fourier transform of f, and $v_o \equiv E_g W/\hbar$. The low-velocity behaviour is thus controlled by the high-frequency asymptotics of the Fourier transform of $V(t)$. The smoothness of the wavefunctions in the convolution (equation (3)) gives rise to short-ranged $\tilde{V}(\omega)$, which defines a distinctive threshold with a sub-power-law behaviour at low velocities. For example, Gaussian smoothness would imply a stopping power (for one only subsystem) going as

$$S \sim \frac{V_o^2}{E_g L}\frac{v_o^2}{v^2} e^{-v_o^2/2v^2} \tag{13}$$

at low v. Figure 1(a) indeed shows the perfect agreement between this expression and the non-perturbative solution of the model for a Gaussian perturbation and $V_o/E_g = 0.002$. It is interesting to note that the peak in this figure happens for $v \sim v_o$, i.e., for $E_g\tau \sim \hbar$, which could have been obtained from uncertainty arguments.

The results above can also be seen in terms of extended states, still within the dispersionless approximation. Assuming, for simplicity in the notation, one Wannier function per unit cell, and thus a lattice vector $\mathbf{R}$ for each i index, the ψ_i (i.e., the $\psi_{\mathbf{R}}$) relate to the $\psi_{\mathbf{k}}$ by a Bloch transformation. Considering crystal momentum conservation, only the $\mathbf{q}$ component of the real-space Fourier transform of $V(\mathbf{r})$ offers a non-zero oscillator strength to transitions between $\mathbf{k}$ and $\mathbf{k}+\mathbf{q}$, and the time dependence being of the form $V(\mathbf{r}-\mathbf{v}t)$ implies that the excitations induced by the moving projectile are such that

$$\mathbf{v}\cdot\mathbf{q} = \omega, \tag{14}$$

with $\omega = E_g/\hbar$ in the dispersionless case. This is illustrated in figure 1(b). Equation (14) is analogous to the expression relating the change in energy with the change in momentum

of a classical particle when colliding with a much more massive particle of velocity **v**: $\mathbf{v}\cdot\Delta\mathbf{p} = \Delta E$. The sum over all transitions satisfying equation (14), with the corresponding oscillator strengths, would yield the same result as before, with the same threshold at low velocities controlled by the tail of the Fourier transform of V.

So reformulated, this analysis can be extended to dispersing bands. In a model direct band gap insulator with parabolic bands for both electrons and holes, as in figure 1(c), the excitation relation in equation (14) implies that any velocity below a critical value will not find allowed excitations. This critical velocity is

$$v_c = \sqrt{\frac{2E_g}{m_e + m_h}}, \tag{15}$$

where m_h and m_e are the effective masses of holes and electrons, respectively. Expressed otherwise, $E_g = \frac{1}{2}m_e v_c^2 + \frac{1}{2}m_h v_c^2$. For lower velocities the stopping power is zero, a definitive threshold.

What happens at the critical velocity is singular, and the kind of singularity depends on the dimensionality in a very similar way as Van Hove singularities in densities of states. In strictly one dimension and assuming a smooth behaviour of the Fourier transform of V, the stopping power would peak before dropping to zero, since at the threshold the excitation line (equation (14)) is tangent to the two parabolas. In higher dimensions, equation (14) defines a hyperplane in the $(\omega, \mathbf{k})$ space with effective excitation slopes $\omega/k \leqslant v$, and thus less dramatic behaviours the higher the dimension. These singularities are weighted by the tail of the Fourier transform of $V(\mathbf{r})$, and thus, any broadening will make them disappear at large $\mathbf{q}$ (low v).

The parabolic bands represent only a very simplified model. A real solid displays bands periodic with $\mathbf{k}$, and thus no matter how slow the projectile moves, equation (14) will still find suitable excitations, still weighted by the tail in the Fourier transform of V. The parabolic model illustrates, however, actual singularities for realistic band structures: critical velocities defined by tangent situations are still possible, as shown in figure 1(d), which induce a substantial drop in the stopping power towards lower velocities, since they are associated to a finite jump to larger $\mathbf{q}$. Interestingly, the low-v asymptotics is affected by such singularities. As can be seen in figure 1(e), infinitesimal changes in slope induce finite jumps in $\mathbf{q}$, the more frequent the lower v. The limit is thus made of singularities superimposed to the tail of the Fourier transform of V.

3.2. Square-potential perturbation

The previous analysis was limited to small perturbing potentials, where the unperturbed band gap E_g dominates the physics. Real projectiles tend to have associated not so small perturbing potentials, which demand non-perturbative analysis. We go back to the dispersionless model.

Before getting into the dynamics of two-state systems with realistic potentials, a very idealized one gives interesting insights. Consider the following square potential,

$$V(t) = \begin{cases} 0 & t < 0, \quad t > \tau \\ V_o & 0 \leqslant t \leqslant \tau, \end{cases} \tag{16}$$

where V_o can be large. The solution is simple. For the duration of the pulse, the Hamiltonian $H_o + V$ has well-defined eigenvectors [$\chi_1(\mathbf{r})$ and $\chi_2(\mathbf{r})$] and eigenvalues (ϵ_1 and ϵ_2) which define the evolution of the system. Expressing the initial state as $\psi_v(\mathbf{r}) = c_1\chi_1(\mathbf{r}) + c_2\chi_1(\mathbf{r})$, its evolution is given by

$$\psi(\mathbf{r}, t) = c_1 e^{-i\epsilon_1 t/\hbar}\chi_1(\mathbf{r}) + c_2 e^{-i\epsilon_2 t/\hbar}\chi_2(\mathbf{r}). \tag{17}$$

By evaluating this expression for $t = \tau$ and re-expressing it in terms of ψ_v and ψ_c, the sought value of β is obtained.

The explicit solution does not bring much to the discussion, except for the following. It is easy to see that equation (17) describes Rabi oscillations of angular frequency $(\epsilon_2-\epsilon_1)/2\hbar$ [10]. After every half period the wavefunction goes back to the initial state, up to a phase (β becomes zero), and therefore if $\tau = 2\pi n\hbar/(\epsilon_2 - \epsilon_1)$ the energy transfer is zero.

Three interesting insights are provided by this result: firstly, the Rabi oscillations in the excitation, i.e., in $c_2(t)$, give rise to oscillations in $\beta(\tau)$ that are trivially identical. It will be shown below how, for arbitrary potentials, $c_2(t)$ describes oscillations that are reminiscent of Rabi oscillations, but which can be quite irregular, while there are quite well-defined *effective* Rabi oscillations in $\beta(\tau)$.

Secondly, it is the *perturbed* band gap $\epsilon_2 - \epsilon_1$ that is the one controlling the stopping (the oscillations), not E_g. This can be related to the perturbation theory results above by noticing that it coincides with the Fourier transform of the $V(t)$ double step function,

$$\tilde{V}(\omega) = V_o \sin(\omega\tau/2)/\omega, \tag{18}$$

evaluated at the perturbed gap. However, an arbitrary $V(t)$ does not define a static perturbed gap, but a time-dependent one, which would only make sense as such in the adiabatic limit, of no interest here. An effective (or average) perturbed band gap can thus be defined from the period of the effective Rabi oscillations.

Thirdly, this potential does not define a threshold at low velocities. The $|\beta(\tau)|$ oscillations mentioned do not decay with large τ, and thus, when plotted versus velocity, $\Delta E = E_g|\beta|^2$ oscillates with constant amplitude and diverging frequency when $v \to 0$. This is equally valid for $V_o \ll E_g$, and thus should be captured by the perturbation analysis above. Indeed, the long range of $\tilde{V}(\omega)$ gives $\Delta E \propto \sin^2(v_o/v)$.

3.3. Numerical solutions: Gaussian perturbation

The case for a more general perturbing potential is studied next by means of the numerical solution of equation (6). The following Gaussian perturbing potential is considered in this section:

$$V(t) = V_o e^{-(t/\tau)^2}, \tag{19}$$

where $\tau \propto 1/v$. Figure 2 displays the main results. The first column shows the time evolution of the transferred energy for different values of V_o and τ. It displays oscillations reminiscent of Rabi oscillations, but very much distorted by the specifics of the potential. More instructive is to plot the final energy transferred, or rather $|\beta|$, versus the characteristic duration of the pulse τ. This is shown in the middle column of figure 2. There are very clean *effective* Rabi oscillations, with a decaying amplitude. For values of V_o equal to or larger than E_g these $|\beta(\tau)|$ oscillations have a remarkably constant frequency. They reflect the number of periods of the oscillations of $|c_2(t)|$ that fit within the scope of the potential, i.e., the frequency observed for $|\beta(\tau)|$ reflects some average frequency of $|c_2(t)|$.

The overall behaviour is approximately captured by

$$|\beta| \sim e^{-(\tau/\tau_o)^\eta} \sin 2\pi \frac{\tau}{T}, \tag{20}$$

at least for $V_o > E_g$. The two upper panels of the middle column in figure 2 show fits to this expression superimposed to the numerical solutions. The fits are barely distinguishable from the data even for $V_o = E_g$. In this regime ($V_o > E_g$), it is observed that $T \propto 1/V_o$, $\tau_o \propto V_o$, and $\eta \to 3/2$. It was shown before that the perturbative limit ($V_o \ll E_g$) for η is 2.

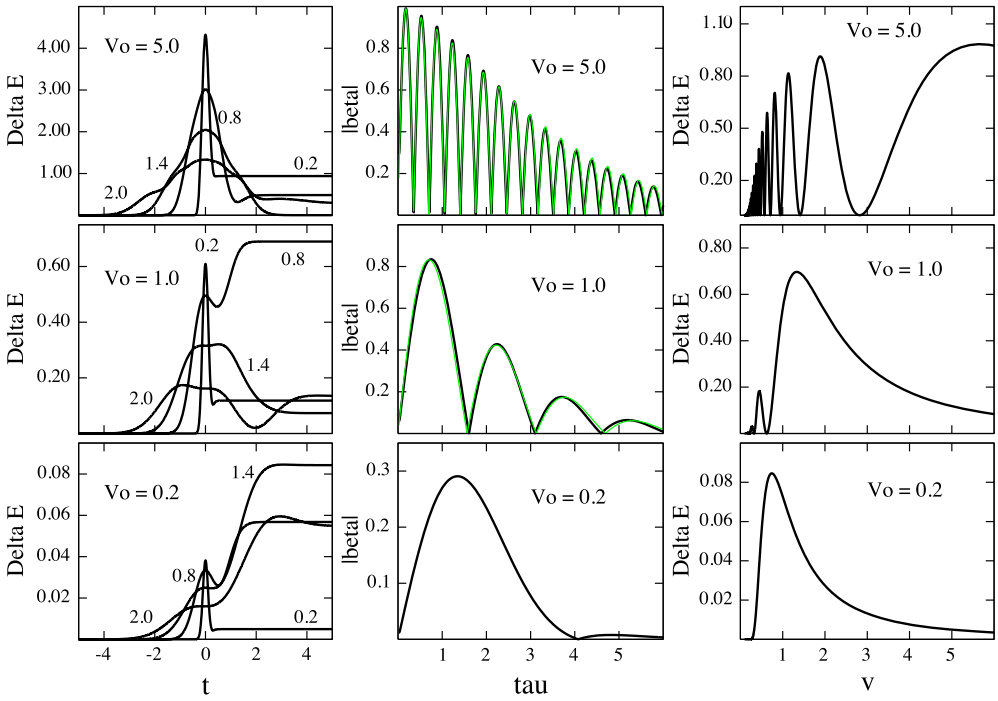

Figure 2. First column: evolution of the excitation energy, $\Delta E(t) = E(t) - E^{\mathrm{BO}}_{\mathrm{G.S.}}(t)$, referring to the Born–Oppenheimer ground-state energy $E^{\mathrm{BO}}_{\mathrm{G.S.}}$, as the projectile passes, for $V_{\mathrm{o}}/E_{\mathrm{g}} = 5.0$, 1.0, and 0.2, in the upper, medium and lower panels, respectively, with graphs for $\tau = 0.2$, 0.8, 1.4, and 2.0, as indicated. Second column: $|\beta|(\tau)$ for the same values of V_{o}. The upper panels compare the numerical solution with the fit with equation (20). Third column: final excitation energy $\Delta E(\infty)$ versus $v = 1/\tau$.

The third column of figure 2 shows the velocity dependence of the transferred energy, analogous to that of the stopping power. The low-V_{o} regime shows the behaviour expected from the perturbation theory analysis above. The effective Rabi oscillations described above for the large-V_{o} regime appear here as oscillations of diverging frequency for $v \to 0$, with an amplitude that defines a threshold going as $\exp[-2(\frac{W}{v\tau_{\mathrm{o}}})^{3/2}]$, only slightly less abrupt than the perturbative one.

The high-velocity limit given by this model corresponds to the $\tau \to 0$ limit, which displays a linear dependence of $|\beta|$ with τ, i.e., a $1/v^2$ dependence of the stopping power at large velocities. It appears quite naturally from this perspective, as the low-τ limit of the sine function in equation (20). The fact that it goes to zero is quite expected, given the fact that the pulse becomes infinitely short (still of V_{o} amplitude). The linear behaviour of $\beta(\tau)$ also seems natural, considering that the amount of effective period covered is proportional to the duration.

4. Conclusions and outlook

A simple model has been used to explore, review and illustrate basic fundamentals of the process of stopping of projectile ions by electrons in a large band gap insulator, with special emphasis on the behaviour at low projectile velocities. Many simplifying assumptions have been made, including the neglect of electronic correlation and self-consistency effects. From

the compared analysis of two different limits, the perturbative $V_o \ll E_g$ and the dispersionless bands limits, the following insights are obtained.

(i) The threshold character at low velocities depends on the smoothness of the convolution of the projectile potential with the local overlap between initial and final states. Well-defined thresholds appear for short-ranged Fourier transforms of that convoluted potential.
(ii) For non-flat bands the threshold becomes highly non-analytical, at least in the perturbative limit, with singular points crowding towards the $v \to 0$ limit.
(iii) Although there are no strict Rabi oscillations in the dynamics related to the passing of an arbitrary potential, effective Rabi oscillations are observed in the dependence of the final energy transferred on the duration of the pulse, for a given projectile potential shape.
(iv) The known dependence on the energy gap E_g of the stopping characteristics for the perturbative limit transforms into a dependence on an average *perturbed* gap.

There are obvious limitations in the model discussed in this work. The oscillations will tend to disappear when the potential is allowed for more than one excitation channel from any given valence state. Also, projectile charge states have not been contemplated here: the projectile can drag electrons, as is obvious for deep core states. More weakly bound electrons are more difficult to treat, and have been considered elsewhere [2, 11, 12]. It also raises issues related to the momentum transferred to electrons, which has been consistently neglected in the context of the dispersionless limit. The model of this work can be easily extended to get qualitative insights into the effects of these other ingredients. However, the necessary introduction of more parameters would render the extended model more difficult to exploit as a simple paradigm.

Other shapes of the projectile potential can also be studied for more quantitative or intermediate studies. More fruitful is the deeper study of the specifics of the low-velocity threshold explicitly exploiting the low-velocity limit. For this purpose, the adiabatic limit can be considered as unperturbed reference, and perturbation theory be used for the deviation from adiabaticity. The dynamic coupling coefficients would allow further qualitative insights into the velocity threshold for insulators. Indeed, the adiabatic theorem [13] immediately suggests a threshold insofar as it predicts negligible excitation when the rate of change of the adiabatic eigenvalues (and thus of the perturbation) is much smaller than the characteristic energy change rate of the system, $\Delta E^2/\hbar$. This is a sufficient condition for low stopping values, but not a necessary one: we saw zero stopping situations related to the width of the pulse. The model presented in this work captures several non-trivial concepts into a very simple paradigm.

Acknowledgments

Discussions with J M Pruneda, J M Pitarke, D Sánchez-Portal, J I Juaristi, A Arnau, and P M Echenique are gratefully acknowledged. Ekhard Salje is thanked for bringing the problem of electronic heating in radiation damage to our attention. EA thanks the Donostia International Physics Centre for its hospitality.

References

[1] Ziegler J F, Biersack J P and Littmark U 1985 *The Stopping and Range of Ions in Matter* (New York: Pergamon)
[2] Echenique P M, Flores F and Ritchie R H 1990 *Solid State Physics* vol 43, ed H Ehrenreich and D Turnbull (New York: Academic) pp 229–308 and references therein
[3] Trachenko K, Dove M T, Artacho E, Todorov I T and Smith W 2006 *Phys. Rev.* B **73** 174207
[4] Trachenko K 2004 *J. Phys.: Condens. Matter* **16** R1491–515 and references therein

[5] Draxler M, Chenakin S P, Markin S N and Bauer P 2005 *Phys. Rev. Lett.* **95** 113201
[6] Pruneda J M, Sánchez-Portal D, Arnau A, Juaristi J I and Artacho E 2007 at press
[7] Lin C D and Martin F 2002 Fast and slow collisions of ions, atoms and molecules *Scattering* ed P Sabatier and E R Pike (London: Academic) and references therein
[8] Runge E and Gross E K U 1984 *Phys. Rev. Lett.* **52** 997
[9] Echenique P M and Ritchie R H 1980 *Phys. Rev.* B **21** 5854
[10] Cohen-Tannoudji C, Diu B and Laloë F 1973 *Mecanique Quantique* (Paris: Hermann) p 412
[11] Guinea F, Flores F and Echenique P M 1982 *Phys. Rev.* B **25** 6109
[12] Närmann A, Monreal R, Echenique P M, Flores F, Heiland W and Schubert S 1990 *Phys. Rev. Lett.* **64** 1601
[13] Marzlin K P and Sanders B C 2004 *Phys. Rev. Lett.* **93** 160408 and references therein